VIP Imaging Agents

DOI: 10.1002/ange.201207131

MRI Visualization of Melanoma Cells by Targeting Overexpressed Sialic Acid with a Gd^{III}-dota-en-pba Imaging Reporter**

Simonetta Geninatti Crich, Diego Alberti, Ibolya Szabo, Silvio Aime, and Kristina Djanashvili**

Altered glycosylation of cell surface proteins and lipids is frequently associated with tumorigenic and metastatic processes.[1] These changes in glycosylation are mainly caused by an increased expression of sialyltransferases, which glycosylate exposed glycans at their terminal positions with anionic monosaccharide sialic acid residues (Sia). Tumor cells overexpressing Sia appear protected against the immune defense system, and as a result, malignancy is increased.[2] Numerous studies have demonstrated that Sia are relevant biomarkers of metastatic activity of tumors,[3] and that the amount of Sia expression on cancer cells correlates with the prognosis of patients.[4] Currently the determination of the sialylation status of solid tumors is carried out on sections of tissue obtained from biopsies. This procedure is not only invasive, it also bears an intrinsic risk that the sample is not representative for the whole, potentially heterogeneous tumor. Therefore, we have investigated probes that are able to noninvasively visualize Sia in vivo.

Macrocyclic or linear lanthanide complexes appear interesting candidates for this intended application, because they can be used either as contrast agents (CA) for magnetic resonance imaging (MRI) or as radiopharmaceuticals for imaging and treatment of tumors. For both tasks, accurate delivery and retention of the complex at the site of disease is mandatory. Previously, we have demonstrated the affinity of ^{160}Tb-dtpa-bisamide (dtpa = diethylenetriamine pentaacetic acid) conjugated to a phenylboronic acid (pba) moiety towards human glioma cells.[5a] The recognition mechanism is based on the reversible formation of five- and six-membered cyclic boronate esters between pba and the exocyclic polyol function of Sia[6] (Scheme 1). Although this type of binding has extensively been exploited for the design of various saccharide sensors[7] and Sia determination assays,[8] its application for in vivo targeting of tumors has not yet been reported. Herein, for the first time, we demonstrate in vivo visualization of tumors by the highly selective dynamic covalent binding between the diol function of overexpressed Sia and a pba-targeting vector conjugated with an MRI reporter (Figure 1).

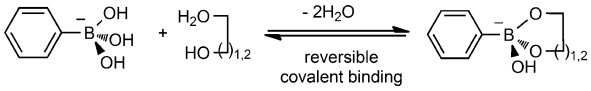

Scheme 1. Formation of the five- and six-membered ring esters from 1,2- or 1,3 diols and phenylboronic acid at physiological pH.

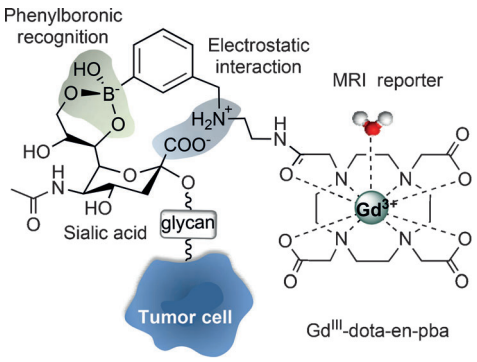

Figure 1. Schematic representation of sialic acid recognition by the imaging reporter Gd^{III}-dota-en-pba through diol–phenylboronic acid interactions on the surface of tumor cells.

The dota chelate (dota = 1,4,7,10-tetraazacyclododecane 1,4,7,10-tetraacetate) has been chosen for the design of the targeting imaging reporter dota-en-pba because of the superior kinetic stability of its complexes with Ln^{III} ions compared to previously reported dtpa-bisamide-pba-complexes.[5,9] The pba group is conjugated via an ethylenediamine (en) spacer. As the amino group of dota-en-pba is positively charged at physiological pH it facilitates the recognition mechanism through electrostatic affinity to the negatively charged carboxylic groups of the Sia residues. The role of this auxiliary interaction has been supported previously by a computer modeling study.[5a]

As Sia expression is directly correlated to melanogenesis, the recognition ability of the designed complex were evaluated on murine melanoma B16-F10 cells. This cell line is commonly used as a well-characterized, highly proliferative tumor model. In melanoma cells, the activity of tyrosinase, the

[*] Dr. S. Geninatti Crich, D. Alberti, I. Szabo, Prof. S. Aime
Department of Chemistry, Molecular Imaging Center
Via Nizza 52, 10126 Turin (Italy)
E-mail: simonetta.geninatti@unito.it
Dr. K. Djanashvili
Department of Biotechnology, Delft University of Technology
Julianalaan 136, 2628 BL, Delft (The Netherlands)
E-mail: k.djanashvili@tudelft.nl

[**] This research was performed in the framework of the EU COST Action TD1004, "Theranostics Imaging and Therapy: an Action to Develop Novel Nanosized Systems for Imaging-Guided Drug Delivery", and supported by Regione Piemonte (PIIMDMT and nano-IGT projects), MIUR (PRIN 2009235JB7). The authors are grateful to Dr. Joop A. Peters for valuable scientific discussions.
dota = 1,4,7,10-tetraazacyclododecane 1,4,7,10-tetraacetate, en = ethylenediamine, pba = phenylboronic acid.

Supporting information for this article is available on the WWW under http://dx.doi.org/10.1002/anie.201207131.

key enzyme for melanogenesis, shows a good correlation with intra- and extracellular Sia levels.[10] This correlation indicates that Sia have an essential role in enzyme expression and, therefore, in the differentiation of melanoma cells. Sialylation/desialylation of some relevant molecules, such as melanosomal sialoglycoconjugates and tyrosinase itself, participate in the regulation of the expression of melanogenic functions. For these reasons, two clones of B16-F10 murine melanoma each characterized by a different phenotype, namely melanogenic (B16-$F10_m$) and nonmelanogenic (B16-$F10_{non}$) cells, have been used to test the pba-based imaging reporter in vitro. The two phenotypes were obtained by growing cells at different pH values. In fact, it is known that B16-F10 cells only form melanin when they are maintained in culture at pH 7.2–7.4.[11] At lower pH melanogenesis is inhibited, whereas other metabolic processes remain almost unaffected. The level of Sia in the B16-$F10_m$ clone was determined to be 3.6 times higher than that in B16-$F10_{non}$; this result is in agreement with previously reported values.[11] The specific binding of Gd^{III}-dota-en-pba to the tumor cells overexpressing Sia was assessed by relaxation rate measurements on the washed cell pellets after incubation with a 0.6 mM solution of the complex for 4 h at 37 °C.

From the results reported in Table 1 it is evident that there is a marked accumulation of the complex at the melanogenic cells that yields high relaxation rates ($R_1 = 1/T_1$), as a result of a higher Gd content, as confirmed by ICP-MS measurements. The relaxation rates are in good correlation with the Sia expression (Figure 2).

To get further insights into the relationship between Gd^{III}-dota-en-pba uptake and the sialylation level/melanogenic activity, B16-F10 cells were incubated for 24 h with a 0.9 mM solution of theophylline, a well-known pigmentation enhancer in murine melanoma cells.[11] As an inhibitor of phosphodiesterase, theophylline has been shown to extensively stimulate pigment production and tyrosinase activity of melanoma cells in vitro. As expected, expression of Sia by the cells preincubated with theophylline increased significantly, thus resulting in accumulation of larger quantities of the Gd complex (Figure 3). This increased binding effect is especially remarkable for the nonmelanogenic cells, as it is 7 times higher than that for the melanogenic cells, thus resulting in a similar level of Sia expression for both cell types. The differences in the Gd levels measured in this experiment compared to the one reported in Table 1 can be explained by the variability of the Sia expression by the B16-F10 cells, as this expression depends on the conditions, that is, pH, composition of medium, number of passages after cell defreezing, etc.

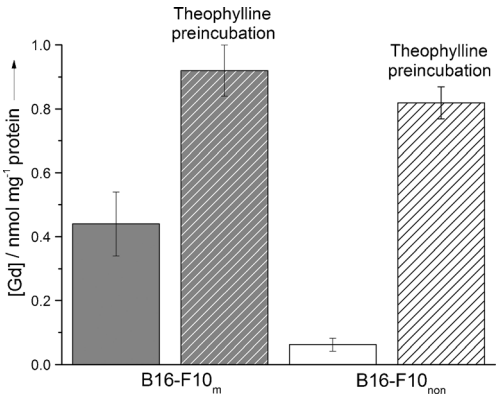

Figure 3. Gd content measured by ICP-MS after incubation of B16-$F10_m$ (grey solid bar) and B16-$F10_{non}$ (white solid bar) cells with Gd^{III}-dota-en-pba, with or without preincubation with theophylline (dashed bars). Error bars have been calculated on the basis of three replicate experiments. Student's *t*-test was used to compare the differences between Gd content before and after theophylline addition. B16-$F10_m$: $P = 0.0015$; B16-$F10_{non\text{-}m}$: $P < 0.0001$. A P value < 0.05 is considered statistically significant.

Table 1: Response of melanogenic and nonmelanogenic cells to the incubation with Gd^{III}-dota-en-pba (0.6 mM, 4 h, 37 °C).

Cell type	R_1^{obs} [s^{-1}]	[Gd] [mol mg^{-1} protein][a]	[Sia] [mol mg^{-1} protein][b]
B16-$F10_m$	0.74 ± 0.03	$1.50\ (\pm 0.5) \times 10^{-9}$	$7.3\ (\pm 0.6) \times 10^{-9}$
B16-$F10_{non\text{-}m}$	0.51 ± 0.04	$0.20\ (\pm 0.5) \times 10^{-9}$	$1.5\ (\pm 0.4) \times 10^{-9}$

[a] Determined by ICP-MS. [b] Determined by AbCAM assay. The data represent the results obtained on the basis of five independent experiments.

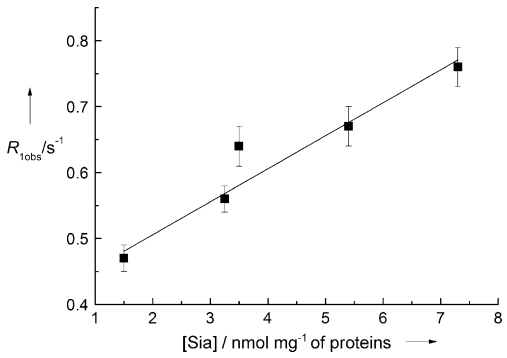

Figure 2. Correlation between sialic acid expression and relaxation rates ($R^2 = 0.9329$) measured in triplicate on cells incubated with Gd^{III}-dota-en-pba.

It is reasonable to assume that successful in vivo tumor targeting, based on the recognition of Sia residues by a pba vector, could be hampered by its competitive binding to glucose in blood (typically present in a concentration of 3.5–5.8 mM). The formation of cyclic esters of pba and glucose is well-documented,[12] and therefore, the interaction of Gd^{III}-dota-en-pba with B16-$F10_m$ cells was evaluated at different concentrations in the presence (5.8 mM) or in the absence of glucose. In both cases, the cells were incubated for 4 h with the complex, after which time the incubation medium was removed, the cells were washed, detached by using EDTA, and the water proton relaxation rates of cell suspensions were measured. As expected, a moderate decrease in the relaxation rates as a result of the competitive binding between the complex and glucose in the medium was observed. However, when the incubation is performed using greater than 1 mM of Gd^{III}-dota-en-pba, the competition effect is negligible. At

these concentrations the amount of the free (not bound to glucose) complex is high enough to saturate all Sia residues available on the cell surface, as demonstrated by the saturating profile of the curve. This observation can be rationalized by the lower affinity of pba to glucose than to Sia.[13] This lower affinity is due to the fact that D(+)glucose is present in solution predominantly (>99%) in its pyranose anomeric form. In this configuration, the diol groups are in an unfavorable position for the formation of pba esters compared to those of Sia, that are positioned on a flexible glycerol tail.[6] The analysis of the relaxation rate behavior in the absence of glucose as a function of the concentration of Gd^{III}-dota-en-pba and the equilibria involved is discussed in the Supporting Information. The probe uptake by cells is also only slightly influenced by the presence of glucose, as demonstrated by MRI images of both melanoma clones (Figure 4B). Melanogenic cells (capillaries 2 and 3) expressing high levels of Sia on their surfaces appear hyperintense on T_1-weighted images compared to nonmelanogenic cells (capillaries 5 and 6). When cells were incubated with the probe in the presence (capillaries 3 and 6) or in the absence (capillaries 2 and 4) of glucose, suspensions containing the same type of cells give images of almost the same intensity, thus demonstrating that glucose has only a minor influence on the binding of Gd^{III}-dota-en-pba to the cells.

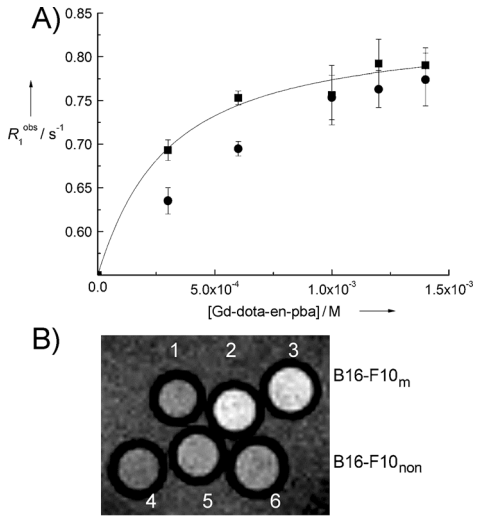

Figure 4. A) Relaxation rates measured for B16-F10 murine melanoma cells, incubated for 4 h at 37°C, with various concentrations of Gd^{III}-dota-en-pba in the presence (circles) or the absence (squares) of glucose (5.8 mM). Detachment of cells by EDTA was applied. The continuous line is the result of the fitting of the data by the equations described in the Supporting Information. B) T_1-weighted spin-echo MR images of agar phantoms containing unlabeled cells (1 and 4) and cells incubated with 0.6 mM Gd^{III}-dota-en-pba in the absence (2 and 4) or in the presence (3 and 6) of 5.5 mM glucose.

Next, in vivo MRI experiments were carried out on mice models bearing a tumor xenograft obtained by subcutaneous injection of approximately 1×10^6 B16-F10$_m$ cells on the right flank. After 8–10 days, the tumor volume was between 20 and 40 mm^3, that is, easily detectable by MRI. Five animals were then intravenously administered with 0.1 mmol kg^{-1} of Gd^{III}-dota-en-pba. A second group of mice ($n=5$) received the same dose of Gd-HPDO3A (a commercial MRI agent with unspecific vascular and extravascular distribution) as control. Fat-suppressed T_1-weighted multislice multiecho MR images were recorded before, 4 h after, and 24 h after contrast agent administration (Figure 5). The analysis of signal intensity (% SI) enhancement measured on the region of interest, which is drawn on the whole tumor regions (see Figure 5), was of 25% and 10% at 4 h and 24 h after the injection of the targeting probe, respectively, whereas no persistent SI was observed for animals injected with the control probe (see the Supporting Information, Figure S1). From Figure 5B, it is apparent that the probe can visualize the heterogeneity of tumor. The % SI enhancement recorded on mice treated with Gd-HPDO3A at the same Gd dose (Figure 5D and Figure S1 in the Supporting Information) was markedly lower and without any significant difference between muscle and tumor regions. Next, to demonstrate the specificity of the binding of Gd^{III}-dota-en-pba to the tumor cells, a competition experiment was performed with Eu^{III}-dota-en-pba, which does not influence the SI in T_1-weighted MR images. A group of four mice were treated with 0.15 mmol kg^{-1} of Eu^{III}-dota-

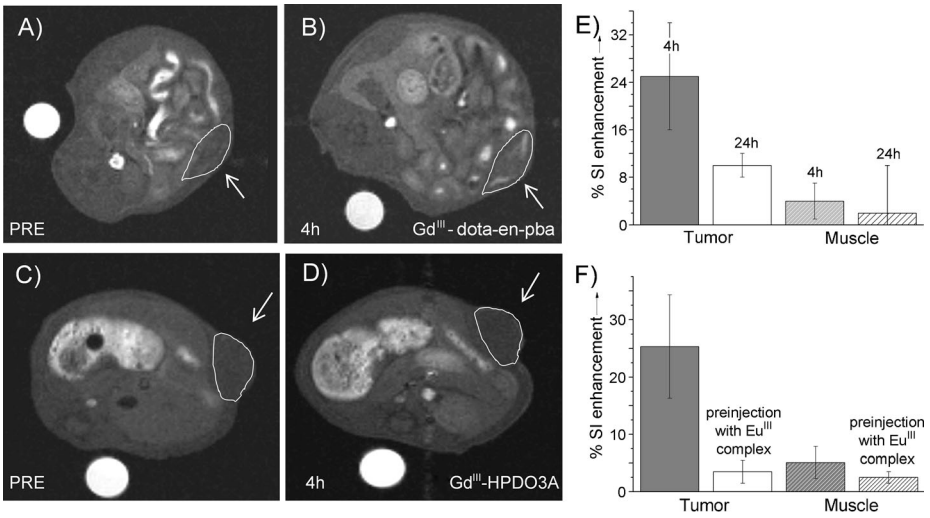

Figure 5. Fat-suppressed T_1-weighted MR spin-echo images of C57BL/6 mice grafted subcutaneously with B16-F10 melanoma cells recorded at 7T before (A) and 4 h after (B) the administration of Gd^{III}-dota-en-pba. For comparison, analogous measurements were performed before (C) and 4 h after (D) the administration of Gd-HPDO3A. The corresponding MRI % SI enhancements (E) were measured in melanoma tumors and muscle 4 h and 24 h after the injection of Gd^{III}-dota-en-pba; the data obtained after injection of Gd^{III}-HPDO3A is reported in the Supporting Information (Figure S1). F) A plot of MRI % SI enhancements measured in melanoma tumor and muscle 4 h after administration of Gd^{III}-dota-en-pba with or without the preinjection with a high dose (0.15 mmol kg^{-1}) of Eu^{III}-dota-en-pba.

en-pba, with subsequent administration of 0.1 mmol kg^{-1} of Gd^{III}-dota-en-pba after 3 h. Figure 5F shows that % SI enhancements measured 4 h after the injection of Gd complex in the region indicated on the whole tumor regions were significantly lower than those measured in the absence of the competitor, thus supporting the view of Gd^{III}-dota-en-pba binding specificity.

In conclusion, we have demonstrated for the first time the feasibility of in vivo tumor targeting based on the recognition of overexpressed sialic acid by a pba-based imaging reporter. The reported results for the murine melanoma tumor could possibly be extended to other tumor types that are known to exhibit high levels of Sia[1] as a function of their metastatic potential, such as breast cancer. The high expression of Sia on the cell surface (approximately 1×10^9/cell) permits their MRI visualization both in vitro and in vivo by using a low molecular weight Gd complex. The use of small-sized targeting contrast agents has evident advantages compared to the use of targeting nanoparticles in terms of their stability, access to the cellular targets, and general toxicity issues. This proof of concept opens new avenues for the design of tumor-specific imaging probes. The prolonged retention of Gd^{III}-dota-en-pba at the tumor site after injection suggests the possibility of using this probe for therapy, provided that a suitable radionuclide is used for labeling the dota-en-pba ligand. Research along these lines is currently under way.

Received: September 3, 2012
Revised: September 26, 2012
Published online: December 6, 2012

Keywords: imaging agents · molecular recognition · phenylboronates · sialic acids · tumor targeting

[1] a) P.-H. Wang, *J. Cancer Mol.* **2005**, *1*, 73 – 81; b) H. Cui, Y. Lin, L. Yue, X. Zhao, J. Liu, *Oncol. Rep.* **2011**, *25*, 1365 – 1371.

[2] a) R. Schauer, *Zoology* **2004**, *107*, 49 – 64; b) R. Kannagi, M. Izawa, T. Koike, K. Miyazaki, N. Kimura, *Cancer Sci.* **2004**, *95*, 377 – 384.

[3] I. M. Duncker, R. Salinas-Marin, C. Martinez-Duncker, *Int. J. Mol. Imaging* **2011**, 283497.

[4] a) A. Cazet, S. Julien, M. Bobowski, M.-A. Krzewinski-Recchi, A. Harduin-Lepers, S. Groux-Degroote, P. Delannoy, *Carbohydr. Res.* **2010**, *345*, 1377 – 1383; b) A. Fernández-Briera, I. Garzia-Parcerio, E. Cuevas, E. Gili-Martin, *Oncology* **2010**, *78*, 196 – 204.

[5] a) K. Djanashvili, G. A. Koning, A. J. G. M. van der Meer, H. T. Wolterbeek, J. A. Peters, *Contrast Media Mol. Imaging* **2007**, *2*, 35 – 41; b) K. Djanashvili, T. L. M. ten Hagen, R. Blangé, D. Schipper, J. A. Peters, G. A. Koning, *Bioorg. Med. Chem.* **2011**, *19*, 1123 – 1130.

[6] K. Djanashvili, L. Frullano, J. A. Peters, *Chem. Eur. J.* **2005**, *11*, 4010 – 4018.

[7] a) J. Ren, R. Trokowski, S. Zhang, C. R. Malloy, A. D. Sherry, *Magn. Reson. Med.* **2008**, *60*, 1047 – 1055; b) S. Aime, M. Botta, W. Dastrú, M. Fasano, M. Panero, *Inorg. Chem.* **1993**, *32*, 2068 – 2071; c) S. Saito, T. L. Massie, T. Maeda, H. Nakazumi, C. L. Colyer, *Sensors* **2012**, *12*, 5420 – 5431; d) Z. Guo, I. Shin, J. Yoon, *Chem. Commun.* **2012**, *48*, 5956 – 5967 (and references therein).

[8] a) A. Matsumoto, H. Cabral, N. Sato, K. Kataoka, Y. Miyahara, *Angew. Chem.* **2010**, *122*, 5626 – 5629; *Angew. Chem. Int. Ed.* **2010**, *49*, 5494 – 5497; b) S. M. Levonis, M. J. Kiefel, T. A. Houston, *Chem. Commun.* **2009**, 2278 – 2280.

[9] C. Cabella, S. G. Crich, D. Corpillo, A. Barge, C. Ghirelli, E. Bruno, V. Lorusso, F. Uggeri, S. Aime, *Contrast Media Mol. Imaging* **2006**, *1*, 23 – 29.

[10] Y. Kinoshita, S. Sato, T. Takeuchi, *Cell Struct. Funct.* **1989**, *14*, 35 – 43.

[11] a) D. C. Bennett, *Environ. Health Perspect.* **1989**, *80*, 49 – 59; b) I. Szabó, S. G. Crich, D. Alberti, F. K. Kálmán, S. Aime, *Chem. Commun.* **2012**, *48*, 2436 – 2438.

[12] E. Battistini, A. Mortillaro, S. Aime, J. A. Peters, *Contrast Media Mol. Imaging* **2007**, *2*, 163 – 171.

[13] a) G. Springsteen, B. Wang, *Tetrahedron* **2002**, *58*, 5291 – 5300; b) M. Regueiro-Figueroa, K. Djanashvili, D. Esteban-Gómez, T. Chauvin, É. Tóth, A. de Blas, T. Rodríguez-Blas, C. Platas-Iglesias, *Inorg. Chem.* **2010**, *49*, 4212 – 4223.

